CORRELATION BETWEEN KINK EFFECT AND FREQUENCY DISPERSION IN PSEUDOMORPHIC HEMTs

J. A. Reynoso-Hernandez[1], R. Plana[2], L. Escotte[2], and J. Graffeuil[2]

[1] CICESE, División de Física Aplicada, Km. 107 Carretera Tijuana-Ensenada, 22860 Ensenada, B. C., Mexico

[2] LAAS-CNRS et Université Paul Sabatier, 7, Av. du Colonel Roche, 31077 Toulouse Cedex, France

ABSTRACT

This paper presents DC and AC frequency dispersion effects of the drain-source output impedance in commercially available pseudomorphic HEMTs. Inductive behaviour observed on the imaginary part of the drain-source impedance is attributed to deep traps in the GaAs substrate from DC and AC measurements versus temperature. On the other hand, DC and AC measurements indicate that kink effect signature is related to impact ionisation at the drain edge of the gate followed by trapping-detrapping processes in the substrate.

INTRODUCTION

Pseudomorphic HEMTs (PHEMTs) are widely used devices for both linear and non-linear microwave circuits due to the enhanced carriers mobility in the InGaAs channel. However, conventional non-linear models do not take into account some spurious effects such as "kink effect" in the DC output characteristics and inductive and/or capacitive behaviours of the AC drain-source impedance in the low frequency range ($f < 10$ MHz).

Kink effect in PHEMTs occurs at low drain-source voltages ($1\ V \leq V_{DS} \leq 3\ V$) at room temperature and is often related to premature breakdown. Trapping and detrapping of carriers from deep levels and/or impact ionisation of carriers could be involved in this mechanism. Previous work reported by Hori and Kuzuhara [1] shows that for MBE AlGaAs/InGaAs PHEMTs hole traps in the AlGaAs layer could be responsible for the kink effect. As for InAlAs/InGaAs/InP HEMTs, Kruppa and Boos [2] suggest that traps located in the InAlAs layer are involved with the kink effect. On the other hand, a two dimensional and theoretical model proposed by Horio and Satoh [3] argues that both impact ionisation and EL2 electron traps located in the SI-GaAs substrate are responsible for the kink effect in MESFETs. However, this model has not been supported by any experimental work yet.

Besides, the frequency dispersion of the output impedance of the devices impacts the design of ultra wide range circuits or on the up-conversion mechanisms (phase noise of microwave oscillators). Up to now, there is a lack of data, especially in terms of the imaginary part of the output impedance frequency dispersion.

In order to get a better understanding of these unwanted effects, this paper reports experimental investigation of both DC conductance and AC output impedance dispersion versus bias and temperature for commercially available pseudomorphic HEMTs.

DC MEASUREMENTS

A set of five commercially available, 100 mil ceramic-packaged, and submicronic AlGaAs/InGaAs/GaAs PHEMTs (MGF4315, $L = 0.35\ \mu m$, $Z = 200\ \mu m$) were used in this work. A DC characterisation was performed consisting in $I_{DS}(V_{DS})$ measurements at different gate-source voltages, V_{GS}, as a function of temperature. From these measurements, the DC output conductance, G_{DS} ($G_{DS} = \partial I_{DS} / \partial V_{DS}$), was derived.

The characteristics $I_{DS}(V_{DS})$ and $I_{GS}(V_{DS})$ are shown in Fig.1, and the output conductance G_{DS} versus V_{DS} from $V_{GS} = -0.4$ V to 0 V at room temperature (294 K) is plotted in Fig. 2. The observed data indicate that below $V_{DS} = 1.5$ V, the output conductance is almost V_{DS} independent. It should be pointed out that G_{DS} decreases when V_{GS} varies from 0 V to -0.4 V which is associated with lower carriers confinement within the InGaAs quantum well. Beyond $V_{DS} = 1.5$ V, at $(V_{DS})^K$ dramatic change in the $G_{DS}(V_{DS})$ plot is observed : the curve exhibits a maximum value representing the kink effect signature. In order to clarify this mechanism, extra DC measurements of output conductance versus temperature, ranging from 294 K to 333 K, were carried out as reported in Fig. 3. The first comment about these experimental data deals with the output conductance decrease as the device is biased at low drain-source voltage values. This behaviour is consistent with carriers mobility degradation in the well. The second comment is related to the output conductance peak magnitude which is reverse dependent of temperature. Furthermore its V_{DS} location shifts towards higher drain-source voltage values with increasing temperature. Both behaviours suggest that impact ionisation process is involved in the kink effect. It is noteworthy from Fig.2 that the peak position shifts in the range of $1.6\ V \leq V_{DS} \leq 2.8\ V$ when the reverse gate-source voltage increases. This behaviour indicates that impact ionisation is located at the drain side of the gate according to [5].

On the other hand, DC characteristics such as $I_{GS}(V_{DS})$ at different V_{GS} bias and temperatures indicate that kink effect does not yield any atypical behaviour. As expected, I_{GS} increases monotonously versus drain-source voltage and decreases when cooling the device. This typical behaviour exclude both hole tunnelling through the valence band barrier to the gate and emission over the top of the valence band barrier to the gate as reported by Heedt *et al.* [6].

DYNAMIC MEASUREMENTS

Dynamic output impedance measurements in the range 20 Hz - 1 MHz were performed under small-signal condition for different temperatures and V_{DS} voltages (before and after the kink effect). A RCL precision meter (HP 4284) was used and an appropriate calibration procedure was carried out in order to avoid package parasitic effects. From dynamic measurements, the real and imaginary part (referred to as $R_{DS}(f)$ and $X_{DS}(f)$) of the output impedance was derived.
Fig.4. shows the real part of the measured output impedance (at 30 °C) at V_{DS} = 1 V and V_{DS} = 2 V (i.e. before and during the kink effect). At 1 MHz, the output resistance $R_{DS}(f)$ at V_{DS} = 2 V is greater than V_{DS} = 1 V. This behaviour can be attributed to hot electrons effect associated with high electric field scattering. Concerning the low frequency range and due to the occurrence of the kink effect, the $R_{DS}(f)$ value at V_{DS}=2V is less than V_{DS} = 1 V.
The imaginary part of the output impedance (at 30 °C) is reported in Fig.5 for the same bias points. Two distinct regions are discernible. The first one is located below 1 kHz and exhibits a capacitive behaviour ($X_{DS}(f) < 0$) featuring a minimum or inverse peak in connection with the time constant of a trapping-detrapping process [4]. The second region occurs at frequencies larger than 1 kHz and indicates an inductive behaviour ($X_{DS}(f) < 0$). An other amplitude peak occurs but is less pronounced with respect to the low frequency one, probably due to the presence of two different processes featuring similar time constants. It should be noted that the amplitude of the peak responsible for the capacitive behaviour decreases when V_{DS} goes from 1 V to 2 V.
Concerning the inductive behaviour, the amplitude of the peak is enhanced during the kink effect. From these observations, it seems that frequency dispersion of the output impedance $Z_{DS}(f)$, attributed to trapping process, and the kink effect are closely correlated.
In order to characterise the trap involved in the kink effect, $Z_{DS}(f)$ measurements versus temperature were performed. Fig.6 and Fig.7 show the variations of $X_{DS}(f)$ for temperature ranging from 30 °C to 70 °C at V_{DS} = 1 V and V_{DS} = 2 V, respectively. The values of the frequency peaks (f_m) associated to capacitive or inductive behaviour are shifted with temperature which is in agreement with thermal activation of deep level traps. The activation energy (E_a) related to each trap is computed from the Arrhenius plot using the following equation :

$$\tau = \frac{1}{2\pi f_m} \approx \frac{1}{T^2}\exp\left(\frac{E_a}{kT}\right)$$

where T is the ambient temperature in Kelvin, τ the time constant of the trap and k the Boltzmann constant. Three distinct activation energies values are extracted from the Arrhenius plot reported on Fig.8. The first one (E_a = 0.6 eV) observed at V_{DS} = 1 V and 2 V is related to the capacitive behaviour. As previously mentioned, two traps with closed time constant are responsible of the inductive behaviour. Nevertheless, only one trap can be extracted at each bias point. At V_{DS} = 1 V, an activation energy of 0.21 eV is determined, which is in agreement with results obtained from low frequency noise measurements [7], while a value of 0.8 eV associated with EL2 center in the GaAs substrate is found at V_{DS} = 2 V. Therefore our results indicate that EL2 centers in the substrate and impact ionisation at the drain edge of the gate are both responsible of the kink effect.

MECHANISM

According to [5], impact ionisation occurs at the drain edge of the gate since $(V_{DS})^K$ increases as reverse gate-source bias $(-V_{GS})$ grows (Fig. 2). As a result of impact ionisation, electrons and holes are created. Most electrons are swept out to the drain giving rise to an increase in the I_{DS} current : this is a first contribution to the kink effect. The remaining few electrons are injected into the SI-GaAs layer. As for holes, they are collected by the gate as well as scattered in the substrate direction. Hence, there is an arrival of both, electrons and holes in the substrate. Assuming that a larger density of arriving holes with respect to that of arriving electrons, a certain amount of holes cannot disappear by recombination and they cannot be evacuated from the substrate since the horizontal electric field is low. Therefore, there is an accumulation of holes in the substrate near the source that implies the substrate potential be decreased. Now, as the potential in the substrate decreases, two processes take place at the same time.
On the one hand, the magnitude of the transversal electric field near the interface InGaAs/GaAs increases. As a consequence, the charge in the quantum well is enhanced and the I_{DS} current increases : this is a second contribution to the kink effect.
On the other hand, due to a weak potential in the substrate, electrons from EL2 traps are released and then, are collected by the drain, inducing an increase in the I_{DS} current : this is a third contribution to the kink effect.

From $I_{DS}(V_{DS})$ and $Z_{DS}(f)$ measurements at various V_{GS} bias and temperatures and with the help of a new technique for deep trap characterisation [4], it can be suggested that three processes are involved in the I_{DS} increase which features the kink effect :

(i) the occurrence of impact ionisation in the drain edge of the gate,
(ii) the increase of the quantum well charge,
(iii) the electrons release from EL2 traps (E_a = 0.8 eV) in the substrate,

the latter processes being, in fact, indirect results of impact ionisation.

CONCLUSION

This paper reports both DC and AC measurements of drain-source output impedance versus bias and ambient temperature on packaged commercially available PHEMTs. Firstly, DC measurements provide the kink effect signature in the 2 V range. Secondly, DC measurements show that impact ionisation process is involved and that holes generated are not evacuated through the gate electrode. From low frequency drain-source output impedance measurements, we demonstrate that an inductive behaviour takes place in the saturation region and is enhanced when the device is biased in the kink effect region due to the impact ionisation mechanism. From output impedance measurements versus temperature, three activation energies of 0.6 eV, 0.21 eV and 0.8 eV have been extracted. The deep level (E_a = 0.8 eV) is observed to be effective at a drain bias corresponding to the kink effect : therefore there is strong evidence that the EL2 center plays a major role in both the kink effect and in the output impedance frequency dispersion.

ACKNOLEDGEMENT

This work was partially supported by a joint funding of the Centre National de la Recherche Scientifique (CNRS, France) and the Consejo Nacional de Ciencia y Tecnología (CONACYT, Mexico). The authors wish to thank J. Rayssac and O. Llopis for assistance during temperature measurements.

REFERENCES

[1] Y. Hori and M. Kuzuhara, "Improved model for kink effect in AlGaAs/InGaAs heterojunction FET's", *IEEE Trans. on Electron Devices*, vol. 41, No. 12, pp. 2262-2267, December 1994.

[2] W. Kruppa and J.B. Boos, "Examination of kink effect in InAlAs/InGaAs/InP HEMT's using sinusoidal and transient excitation", *IEEE Trans. on Electron Devices*, vol. 42, No. 10, pp. 1717-1723, October 1995.

[3] K. Horio and K. Satoh, "Two-dimensional analysis of substrate-related kink phenomena in GaAs MESFET's", *IEEE Trans. on Electron Devices*, vol. 41, No. 12, pp. 2256-2261, December 1994.

[4] J.A. Reynoso-Hernandez, L. Escotte, R. Plana, and J. Graffeuil, "Deep level characterisation in GaAs FETs by means of the frequency dispersion of the output impedance", *Electron. Lett.*, vol. 31, No. 8, pp. 677-678, 13th April 1995.

[5] J. Haruyama and H. Katano, "Impact ionisation in GaAs metal-semiconductor field-effect transistors with a lightly doped drain structure and an $Al_{0.2}Ga_{0.8}As$/GaAs heterobuffer layer", *J. Appl. Phys.*, vol. 77, No. 8, pp. 3913-3918, 15 April 1995.

[6] C. Heedt, F. Buchali, W. Prost, W. Brockerhoff, D. Fritzsche, H. Nickel, R. Losch, W. Schlapp and F.J. Tegude "Drastic reduction of gate leakage in InAlAs/InGaAs HEMT's Using a Pseudomorphic InAlAs Hole Barrier Layer", *IEEE Trans. on Electron Devices, vol. 41, no 10, pp 1685-1689, Oct 1994.*

[7] R. Plana, L. Escotte, O. Llopis, H. Amine, T. Parra, M. Gayral and J. Graffeuil, "Noise in AlGaAs/InGaAs/GaAs pseudomorphic HEMT's from 10 Hz to 18 GHz", *IEEE Trans. on Electron Devices, vol. 40, no 5, pp 852-858, May 1995.*

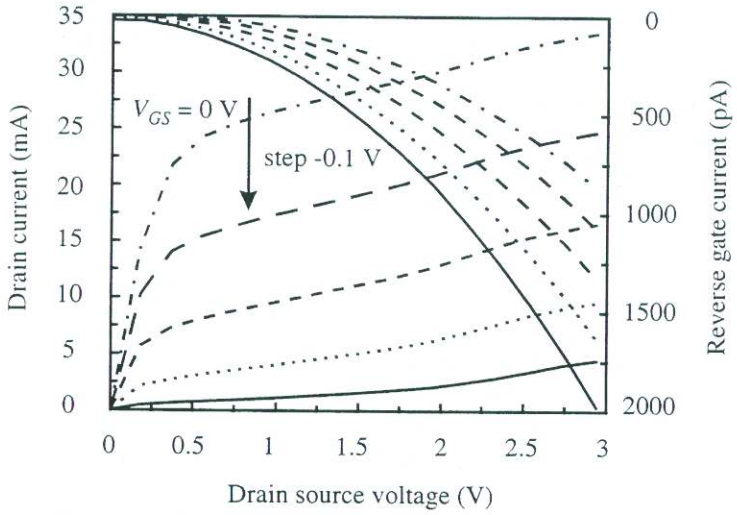

Fig 1 : I_{DS}-V_{DS} and I_{GS}-V_{DS} characteristics at different V_{GS} values.

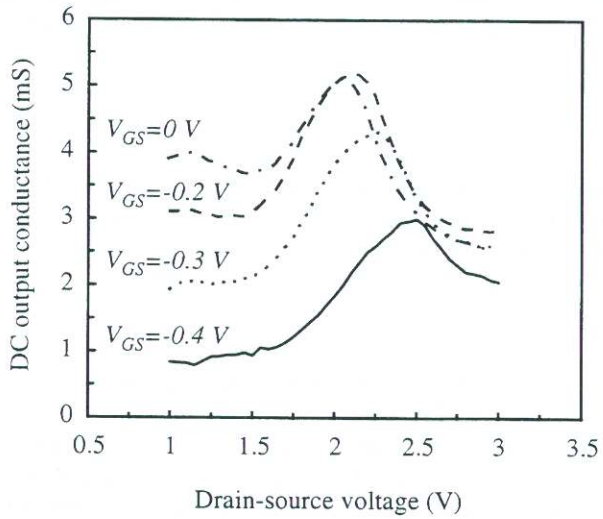

Fig. 2 : $G_{DS}(V_{DS})$ characteristics at different V_{GS} values and at room temperature for a PHEMT.

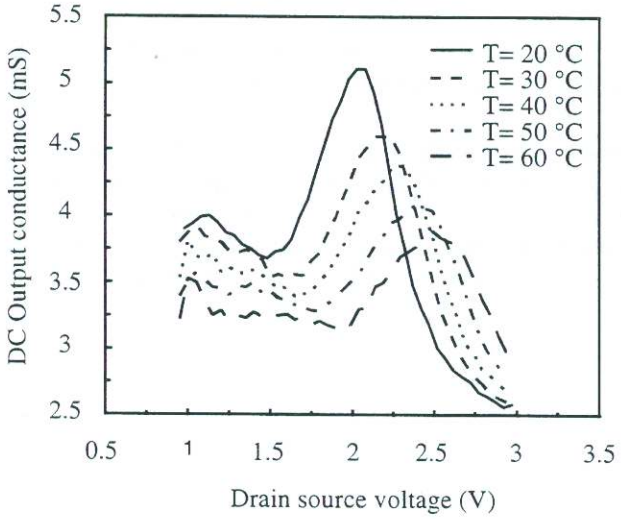

Fig. 3 : Temperature dependence of $G_{DS}(V_{DS})$ characteristics at V_{GS} = 0 V for a PHEMT.

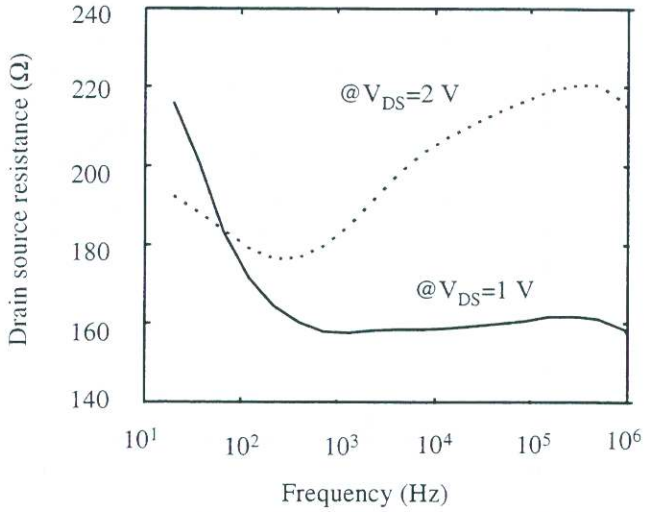

Fig. 4 : Drain-source resistance $R_{DS}(f)$ versus frequency for a PHEMT biased at $V_{GS} = 0$ V.

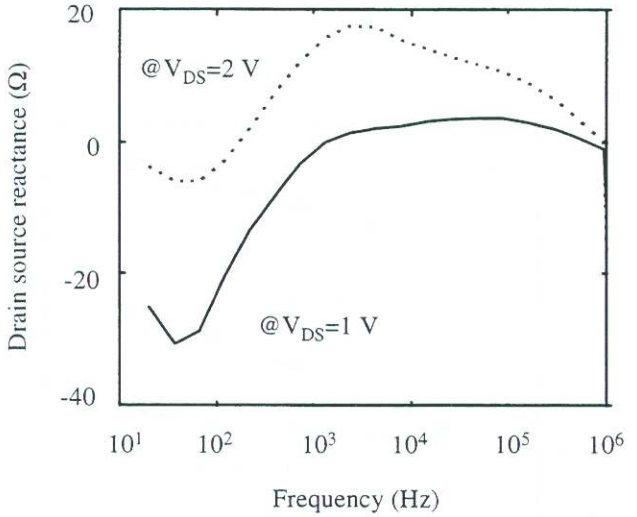

Fig. 5 : Drain-source reactance $X_{DS}(f)$ versus frequency for a PHEMT biased at $V_{GS} = 0$ V.

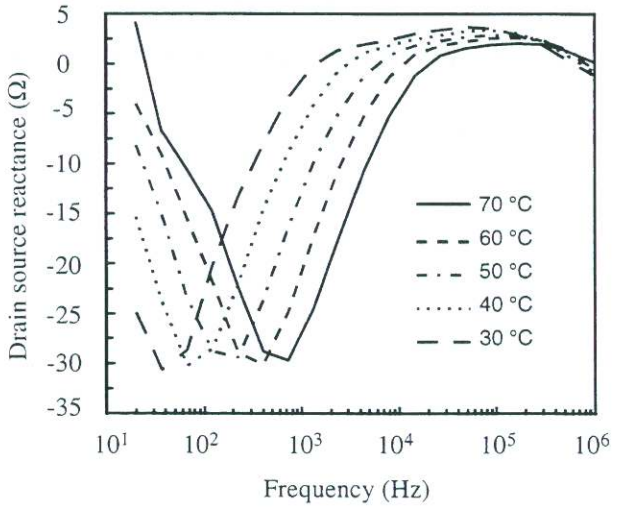

Fig. 6 : Temperature dependence of drain-source reactance $X_{DS}(f)$ versus frequency for a PHEMT biased at $V_{DS} = 1$ V and $V_{GS} = 0$ V.

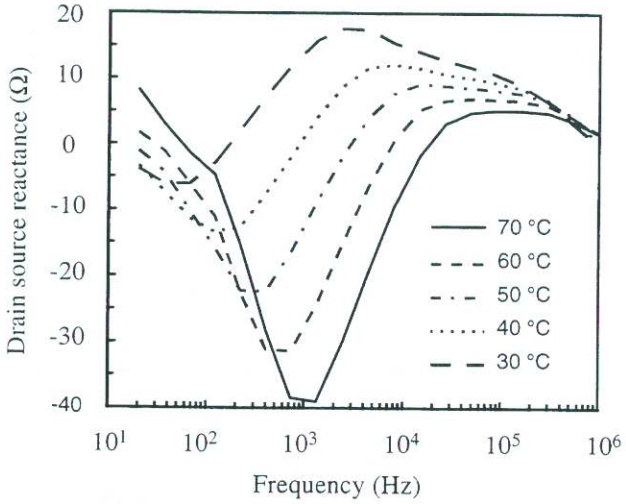

Fig. 7 : Temperature dependence of drain-source reactance $X_{DS}(f)$ versus frequency for a PHEMT biased at $V_{DS} = 2$ V and $V_{GS} = 0$ V.

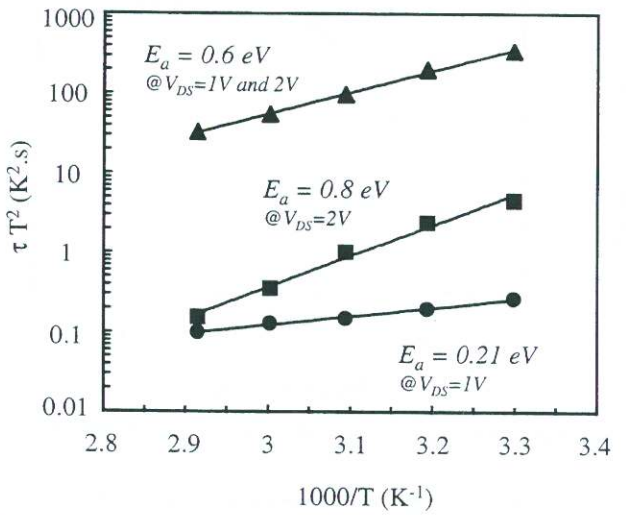

Fig. 8 : Arrhenius plot for extraction of trap activation energy.